

Rapid Solar Sail Rendezvous Missions to Asteroid 99942 Apophis

Giovanni Mengali* and Alessandro A. Quarta†

University of Pisa, 56122 Pisa, Italy

DOI: 10.2514/1.37141

Different concepts for eliminating the threat of collision with a near-Earth object have been suggested in recent years. Most of them require that a probe is inserted in orbit around the object to obtain accurate physical and orbital data. Asteroid 99942 Apophis is a member of the Aten group of asteroids, having orbital periods shorter than 1 year. Such an asteroid is used here as a practical example to investigate the characteristics of new mission concepts and as a candidate for a potential space agency project aimed to tag an asteroid either for scientific purposes or for a deflection mission decision. The purpose of this paper is to investigate the potentialities offered by a solar-sail-based rendezvous mission toward Apophis. In particular, rapid transfer trajectories are studied, that is, missions whose transfer times are less than one terrestrial year. We show that a realistic near-term mission option, with a transfer time of about 300 days, requires a solar sail with a characteristic acceleration of 0.5 mm/s^2 . A square solar sail with a side of about 90 m is needed for a payload of 50 kg, whereas a greater sail with a side of 160 m is called for with a payload of 150 kg. The solar sail performance is compared to that achievable with conventional propulsion systems.

Nomenclature

| | | |
|--------------------|---|----------------------------------------------------------------------------------------|
| A_{ij} | = | generic entry of matrix A |
| a | = | semimajor axis, astronomical unit |
| a_c | = | characteristic acceleration, mm/s^2 |
| \mathbf{a}_s | = | solar radiation pressure acceleration, mm/s^2 |
| b_1, b_2, b_3 | = | force coefficients |
| \mathbf{c} | = | vector, days^{-1} |
| e | = | orbital eccentricity |
| f, g, h, k | = | modified equinoctial elements |
| H | = | Hamiltonian |
| I_{sp} | = | specific impulse, s |
| i | = | orbital inclination, deg |
| $\hat{\mathbf{i}}$ | = | unit vector |
| L | = | true longitude, deg |
| m | = | total sailcraft mass, kg |
| m_{pay} | = | payload mass, kg |
| m_s | = | sail film/structure mass, kg |
| $\hat{\mathbf{n}}$ | = | unit vector normal to the sail |
| p | = | semilatus rectum, astronomical unit |
| \mathbf{r} | = | sun–spacecraft position vector ($r \triangleq \ \mathbf{r}\ $), astronomical unit |
| S | = | sail area, m^2 |
| T | = | thrust, mN |
| t | = | time, days |
| \mathbf{u} | = | control vector, deg |
| \mathbf{v} | = | velocity vector, km/s |
| \mathbf{x} | = | state vector |
| α | = | sail cone angle, deg |
| β_σ | = | dimensionless sail loading |
| Δt | = | flight time, days |
| δ | = | sail clock angle, deg |
| λ | = | adjoint vector |
| μ | = | gravitational parameter, km^3/s^2 |

| | | |
|------------------|---|--------------------------------------------|
| ν | = | true anomaly, deg |
| $\tilde{\sigma}$ | = | reference sail loading, g/m^2 |
| σ_s | = | sail assembly loading, g/m^2 |
| Ω | = | right ascension of the ascending node, deg |
| ω | = | argument of pericenter, deg |

Subscripts

| | | |
|------------|---|---------------|
| f | = | final |
| max | = | maximum |
| 0 | = | initial |
| \oplus | = | Earth |
| \odot | = | sun |
| \diamond | = | 99942 Apophis |

Superscripts

| | | |
|---------|---|-----------------|
| T | = | transpose |
| \cdot | = | time derivative |

Introduction

ONE of the most unpredictable risks for public health and Earth environment is the threat posed by near-Earth objects (NEOs), that is, by small celestial bodies with a perihelion of less than 1.3 AU (astronomical unit). Although the impact of objects smaller than 50 mm in diameter with Earth's atmosphere happens frequently every year, in most cases, they burn up and get destroyed before reaching the Earth's surface [1]. On occasion, however, a somewhat larger object is able to penetrate the atmosphere. The most catastrophic of such events in modern history is usually referred to as the Tunguska explosion, which occurred near Tunguska, Siberia, on 30 June 1908 [2]. That explosion, with an energy level of 10–15 megatons of TNT, was likely caused by the air burst of a large meteoroid or comet fragment at an altitude of 5–10 km above Earth's surface and was able to destroy essentially everything within a 25-km radius.

Usually, the potential threat posed by NEOs is classified with the aid of the Torino scale,[‡] which assigns a number to the likelihood that an asteroid will collide with Earth. Zero and one means virtually no chance of impact or damage, 10 means certain catastrophe. Until the end of 2004, no object had ever been given a rating higher than one. Still, on 23 December 2004, an asteroid referred to as 99942 Apophis

Received 14 February 2008; revision received 2 September 2008; accepted for publication 22 September 2008. Copyright © 2008 by G. Mengali and A. A. Quarta. Published by the American Institute of Aeronautics and Astronautics, Inc., with permission. Copies of this paper may be made for personal or internal use, on condition that the copier pay the \$10.00 per-copy fee to the Copyright Clearance Center, Inc., 222 Rosewood Drive, Danvers, MA 01923; include the code 0022-4650/09 \$10.00 in correspondence with the CCC.

*Associate Professor, Department of Aerospace Engineering; g.mengali@ing.unipi.it. Member AIAA.

†Research Assistant, Department of Aerospace Engineering; a.quarta@ing.unipi.it. Member AIAA.

[‡]For a definition, see http://neo.jpl.nasa.gov/torino_scale.html.

was given a rating of two, and, four days later, the level was raised to four. Subsequent measurements have substantially reassessed the impact risk, and Apophis is now expected to make a close approach to Earth without threatening collision on 13 April 2029. On that occasion, however, the Earth will deflect Apophis's orbit in such a way that a small possibility exists of an impact with Earth during a second encounter in 2036. Although current estimates rate the probability of impact as very low, Apophis is being used as an example to enable design of a broader type of mission to any potentially dangerous asteroid. In particular, in 2007, the Planetary Society promoted a competition[§] aiming at analyzing different missions whose purpose is to send a spacecraft near the asteroid. In fact, tagging the asteroid may be necessary to track Apophis accurately enough to determine whether it will impact Earth, and thus help decide whether to mount a deflection mission to alter its orbit.

In the mission scenario suggested by the Planetary Society, the spacecraft must be able to reach Apophis within 2017, thus giving sufficient time for a deflection mission decision (enabling 3 years development for a deflection mission and 9 years to rendezvous and deflect it). Assuming such a requirement, in this paper, we study the potentialities offered by a solar sail spacecraft to fulfil the rendezvous mission. In particular, rapid transfer trajectories are investigated, that is, missions whose transfer times are less than one terrestrial year. The paper aims at emphasizing the relationships between sail performance (in terms of characteristic acceleration) and mission time. As a result, the best performance characteristics necessary to fulfil the mission are found, along with the corresponding available launch windows.

Mathematical Model

The equations of motion for a flat solar sail, of mass m and area S , in a Cartesian heliocentric inertial frame $\mathcal{T}_\odot(\hat{\mathbf{i}}_x, \hat{\mathbf{i}}_y, \hat{\mathbf{i}}_z)$ are

$$\dot{\mathbf{r}} = \mathbf{v} \quad (1)$$

$$\dot{\mathbf{v}} = -\frac{\mu_\odot}{r^3} \mathbf{r} + \mathbf{a}_s \quad (2)$$

where \mathbf{r} and \mathbf{v} are the spacecraft position and velocity, and \mathbf{a}_s is the sailcraft acceleration due to the solar radiation pressure. Assuming a nonperfect reflection model, the propulsive acceleration \mathbf{a}_s at a distance r from the sun is given by [3]

$$\mathbf{a}_s = \frac{\beta_\sigma \mu_\odot}{2r^2} (\hat{\mathbf{r}} \cdot \hat{\mathbf{n}}) [b_1 \hat{\mathbf{r}} + (b_2 \hat{\mathbf{r}} \cdot \hat{\mathbf{n}} + b_3) \hat{\mathbf{n}}] \quad (3)$$

where $\beta_\sigma \triangleq \tilde{\sigma}/(m/S)$ is the dimensionless sail loading [4] with $\tilde{\sigma} \triangleq 1.539 \text{ g/m}^2$. Also, b_1 , b_2 , and b_3 are the dimensionless force coefficients related to the thermo-optical properties of the reflective film, $\hat{\mathbf{r}} \triangleq \mathbf{r}/r$ is the unit radial vector, and $\hat{\mathbf{n}}$ is the unit vector normal to the sail in a direction such that $\hat{\mathbf{r}} \cdot \hat{\mathbf{n}} > 0$.

In most cases the performance of a solar sail is quantified through the characteristic acceleration a_c , that is, the acceleration experienced by a solar sail whose reference plane is oriented perpendicular to the solar rays (i.e., $\hat{\mathbf{r}} \equiv \hat{\mathbf{n}}$) at a distance $r_0 \triangleq 1 \text{ AU}$. From Eq. (3), it is found that

$$a_c = \frac{(b_1 + b_2 + b_3) \beta_\sigma \mu_\odot}{2r_0^2} \quad (4)$$

For a perfectly reflecting (ideal) solar sail, $b_1 + b_2 + b_3 = 2$, and Eq. (4) reduces to $a_c = \beta_\sigma \mu_\odot / r_0^2$. The optical force model for a sail with a highly reflective aluminum-coated front side and a highly emissive chromium-coated back side is, instead, characterized by the coefficients [3] $b_1 = 0.1728$, $b_2 = 1.6544$, and $b_3 = -0.0109$.

For numerical simulation purposes, it is useful to introduce the vector \mathbf{x} of modified equinoctial elements [5,6], defined as

$$\mathbf{x} \triangleq [p, f, g, h, k, L]^T \quad (5)$$

As a result [7], the equations of motion (1) and (2) become

$$\dot{\mathbf{x}} = \mathbf{A} \mathbf{x} + \mathbf{c} \quad (6)$$

where

$$\mathbf{c} \triangleq \left[0, 0, 0, 0, 0, \sqrt{\mu_\odot p} \left(\frac{1 + f \cos L + g \sin L}{p} \right)^2 \right]^T \quad (7)$$

and $\mathbf{A} \in \mathbb{R}^{6 \times 3}$ is a suitable matrix whose generic entry will be referred to as A_{ij} . It may be shown [7] that $A_{11} = A_{13} = A_{41} = A_{42} = A_{51} = A_{52} = A_{61} = A_{62} = 0$, whereas

$$A_{12} = \frac{2p}{1 + f \cos L + g \sin L} \sqrt{\frac{p}{\mu_\odot}} \quad (8)$$

$$A_{21} = \sin L \sqrt{\frac{p}{\mu_\odot}} \quad (9)$$

$$A_{22} = \frac{(2 + f \cos L + g \sin L) \cos L + f}{1 + f \cos L + g \sin L} \sqrt{\frac{p}{\mu_\odot}} \quad (10)$$

$$A_{23} = -\frac{g(h \sin L - k \cos L)}{1 + f \cos L + g \sin L} \sqrt{\frac{p}{\mu_\odot}} \quad (11)$$

$$A_{31} = -\cos L \sqrt{\frac{p}{\mu_\odot}} \quad (12)$$

$$A_{32} = \frac{(2 + f \cos L + g \sin L) \sin L + g}{1 + f \cos L + g \sin L} \sqrt{\frac{p}{\mu_\odot}} \quad (13)$$

$$A_{33} = \frac{f(h \sin L - k \cos L)}{1 + f \cos L + g \sin L} \sqrt{\frac{p}{\mu_\odot}} \quad (14)$$

$$A_{43} = \frac{(1 + h^2 + k^2) \cos L}{2(1 + f \cos L + g \sin L)} \sqrt{\frac{p}{\mu_\odot}} \quad (15)$$

$$A_{53} = \frac{(1 + h^2 + k^2) \sin L}{2(1 + f \cos L + g \sin L)} \sqrt{\frac{p}{\mu_\odot}} \quad (16)$$

$$A_{63} = \frac{h \sin L - k \cos L}{1 + f \cos L + g \sin L} \sqrt{\frac{p}{\mu_\odot}} \quad (17)$$

For the sake of completeness, the Appendix summarizes the transformations from modified equinoctial elements to classical orbital elements (a , e , i , Ω , ω , and ν) and to the sailcraft position and velocity components (the latter being calculated with respect to \mathcal{T}_\odot). Note that the sun-sailcraft distance r , required for the calculation of the gravitational and propulsive acceleration in Eqs. (2) and (3), can be written in terms of modified equinoctial elements as

$$r = \frac{p}{1 + f \cos L + g \sin L} \quad (18)$$

The introduction of the modified equinoctial elements into the

[§]See http://www.planetary.org/programs/projects/apophis_competition/.

equations of motion allows one to significantly reduce the computational time necessary for the solar sail trajectory integration. Moreover, the presence of the true longitude L in the set of the state variables is useful for simplifying the analytic approach of the optimal control problem that will be discussed in the next section.

Consider now a rotating radial–tangential–normal (RTN) $\mathcal{T}_{\text{RTN}}(\hat{\mathbf{i}}_R, \hat{\mathbf{i}}_T, \hat{\mathbf{i}}_N)$ coordinate frame [7] whose unit vectors are

$$\hat{\mathbf{i}}_R = \frac{\mathbf{r}}{r}, \quad \hat{\mathbf{i}}_N = \frac{\mathbf{r} \times \mathbf{v}}{\|\mathbf{r} \times \mathbf{v}\|}, \quad \hat{\mathbf{i}}_T = \hat{\mathbf{i}}_N \times \hat{\mathbf{i}}_R \quad (19)$$

The orientation of $\hat{\mathbf{n}}$ in the rotating frame \mathcal{T}_{RTN} is unambiguously characterized by means of the cone angle $\alpha \in [0, \pi/2]$ and the clock angle $\delta \in [-\pi, \pi]$ (see Fig. 1) as [8]

$$[\hat{\mathbf{n}}]_{\mathcal{T}_{\text{RTN}}} = [\cos \alpha, \sin \alpha \cos \delta, \sin \alpha \sin \delta]^T \quad (20)$$

Substituting Eq. (20) into Eq. (3), one obtains the propulsive acceleration components in the rotating frame

$$[\mathbf{a}_s]_{\mathcal{T}_{\text{RTN}}} = \frac{\beta_\sigma \mu_\odot}{2r^2} \cos \alpha \begin{bmatrix} b_1 + (b_2 \cos \alpha + b_3) \cos \alpha \\ (b_2 \cos \alpha + b_3) \sin \alpha \cos \delta \\ (b_2 \cos \alpha + b_3) \sin \alpha \sin \delta \end{bmatrix} \quad (21)$$

where r depends on the equinoctial elements according to Eq. (18). Finally, substituting Eq. (21) into Eq. (6), the spacecraft dynamics can be described through six first-order nonlinear differential equations that can be formally written as

$$\dot{\mathbf{x}} = \mathbf{f}(\mathbf{x}, \mathbf{u}) \quad (22)$$

where

$$\mathbf{u} \triangleq [\alpha, \delta]^T \quad (23)$$

represents the solar sail control vector.

Problem Statement

In this paper, we are mainly interested in calculating the minimum time trajectories that allow a sailcraft to optimally rendezvous with Apophis. For all of the trajectories within this paper, a sail optical force model is assumed, along with a direct interplanetary insertion of the sailcraft at Earth with zero hyperbolic excess energy (launch $C_3 \equiv 0 \text{ km}^2/\text{s}^2$). In fact, the effect of a C_3 value different from zero can be taken into account only provided that the characteristics of the launch system, which is used to escape from the Earth, are given [9]. Nevertheless, the condition $C_3 \equiv 0 \text{ km}^2/\text{s}^2$, which is representative of a solar sail deployment on a parabolic Earth escape trajectory, provides conservative results as long as the rendezvous flight time is concerned.

In mathematical terms, the problem is to find the optimal control law $\mathbf{u}(t)$ (where $t \in [0, t_f]$), which minimizes the time t_f necessary to transfer the spacecraft from an initial \mathbf{x}_0 to a final \mathbf{x}_f prescribed state. This amounts to maximizing the performance index:

$$J = -t_f \quad (24)$$

Using an indirect approach, from Eq. (6), the Hamiltonian of the system is

$$H \triangleq (\mathbf{A}\mathbf{a}_s) \cdot \boldsymbol{\lambda} + \mathbf{c} \cdot \boldsymbol{\lambda} \quad (25)$$

where $\boldsymbol{\lambda} \triangleq [\lambda_p, \lambda_f, \lambda_g, \lambda_h, \lambda_k, \lambda_L]^T$ is the adjoint vector whose time derivative is given by the Euler–Lagrange equation:

$$\dot{\boldsymbol{\lambda}} = -\frac{\partial H}{\partial \mathbf{x}} \quad (26)$$

The explicit expression of the Euler–Lagrange equation is rather involved and is not reported here for the sake of conciseness. The optimal value of the control angles α and δ is obtained by invoking the Pontryagin’s maximum principle, that is, by maximizing, at any time, the Hamiltonian H given by Eq. (25). In particular, as long as

the clock angle δ is concerned, by imposing the necessary condition $\partial H / \partial \delta = 0$, one obtains [10]

$$\sin \delta = A_{23}\lambda_f + A_{33}\lambda_g + A_{43}\lambda_h + A_{53}\lambda_k + A_{63}\lambda_L \quad (27)$$

$$\cos \delta = A_{32}\lambda_g + A_{12}\lambda_p + A_{22}\lambda_f \quad (28)$$

where the terms A_{ij} are defined in Eqs. (8–17). On the other hand, the second necessary condition $\partial H / \partial \alpha = 0$ does not provide a closed-form solution for the clock angle α . Therefore, the maximization of H with respect to α is performed by means of a numerical algorithm based on golden section search and parabolic interpolation [11].

The boundary-value problem associated with the variational problem is constituted by the equation of motion (22) and by the Euler–Lagrange Eq. (26). The corresponding 12 boundary conditions are related to the desired spacecraft position and velocity at the initial t_0 and final t_f time. The transversality condition $H(t_f) = 1$, needed to determine the value of t_f , completes the differential problem [10]. In all of the simulations, the differential equations have been integrated in double precision using a variable order Adams–Bashforth–Moulton solver with absolute and relative errors of 10^{-10} . The boundary-value problem has been solved by means of a hybrid numerical technique that combines the use of genetic algorithms to obtain a rough estimate of the adjoint variables, with gradient-based and direct methods to refine the solution [3].

Simulation Results

The problem is addressed in three steps. First, the theoretically optimal performance is sought as a function of the solar sail characteristic acceleration. This corresponds to solving an optimal orbit-to-orbit transfer without ephemeris constraints. Second, for a given annual position of Earth (or launch date), the minimum transfer times toward Apophis’s orbit are found. The outputs of this second phase are then used in the third step to calculate the most promising launch windows for a selected value of solar sail characteristic acceleration [or β_σ , see Eq. (4)].

Orbit-to-Orbit Transfer

As stated, the minimum time orbit-to-orbit transfer problem is solved first, with both initial and final true longitude left free. As a result, the more advantageous relative starting positions between Earth and Apophis are found. Note that the minimum orbit-to-orbit transfer times are obtained as an output of the optimization process.

In our mission scenario, in which both Earth and Apophis are assumed to follow conic orbits around the sun, the 12 boundary conditions are

$$p(t_0) = p_\oplus, \quad f(t_0) = f_\oplus, \quad g(t_0) = g_\oplus \quad (29)$$

$$h(t_0) = h_\oplus, \quad k(t_0) = k_\oplus, \quad \lambda_L(t_0) = 0$$

$$p(t_f) = p_\odot, \quad f(t_f) = f_\odot, \quad g(t_f) = g_\odot \quad (30)$$

$$h(t_f) = h_\odot, \quad k(t_f) = k_\odot, \quad \lambda_L(t_f) = 0$$

The orbital parameters corresponding to the date 1 January 2013 (calculated with the JPL DE405 ephemerides model [12,13]) are summarized in Table 1.

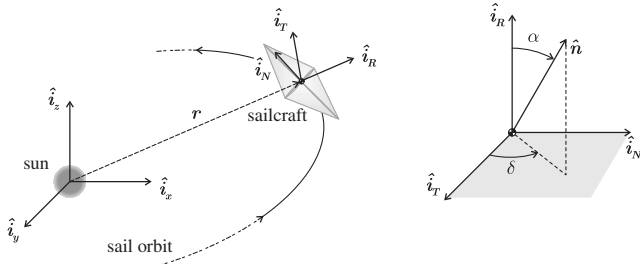
The mission times are shown in Fig. 2a, whereas the corresponding sailcraft initial and final position [in terms of true anomaly ν , see Eq. (A8)] are illustrated in Fig. 2b. As shown in Fig. 2a, characteristic accelerations less than about 0.4 mm/s^2 are inadequate for a rapid orbital transfer, because the corresponding optimal mission time would be greater than 1 year. Assuming, for example, a characteristic acceleration $a_c = 0.5 \text{ mm/s}^2$, the minimum mission time is 250 days and the initial sailcraft position, measured on Earth’s orbit, is $\nu_0 = 230^\circ$ (this corresponds to an end-of-August launch), whereas the final position on Apophis’s orbit is $\nu_f = 220^\circ$.

Table 1 Modified equinoctial orbital elements evaluated at 01 January 2013

| Body | p , AU | f | g | h | k |
|---------|----------|---------------------------|---------------------------|---------------------------|---------------------------|
| Earth | 0.99908 | -3.35075×10^{-3} | 1.57132×10^{-2} | -1.39364×10^{-5} | 1.39334×10^{-6} |
| Apophis | 0.88835 | 0.16689 | -9.34515×10^{-2} | -2.64779×10^{-2} | -1.19829×10^{-2} |

Minimum Transfer Times

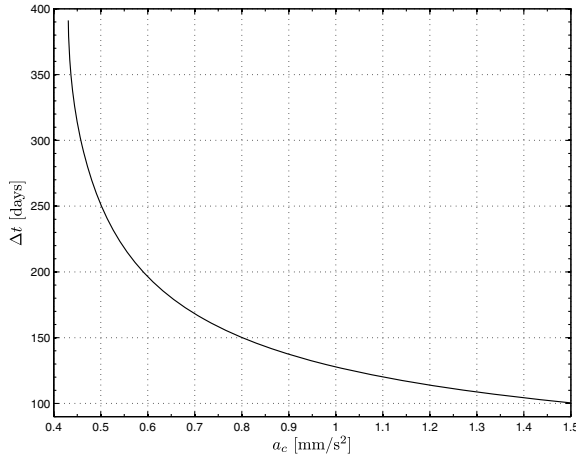
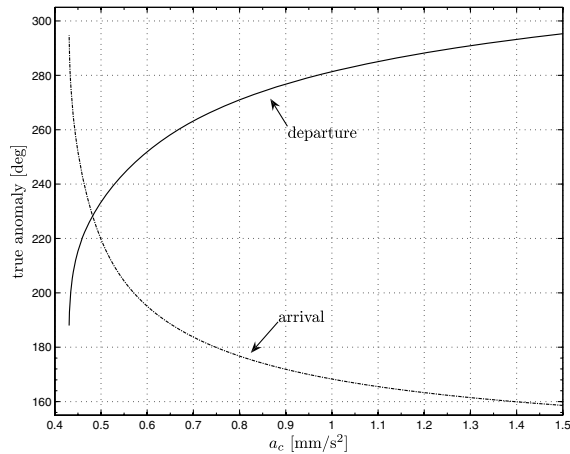
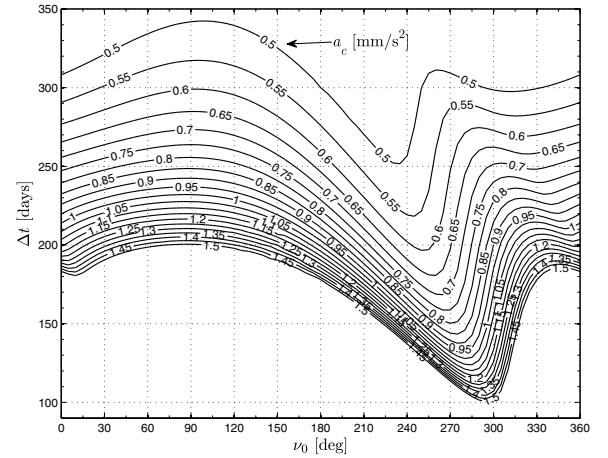
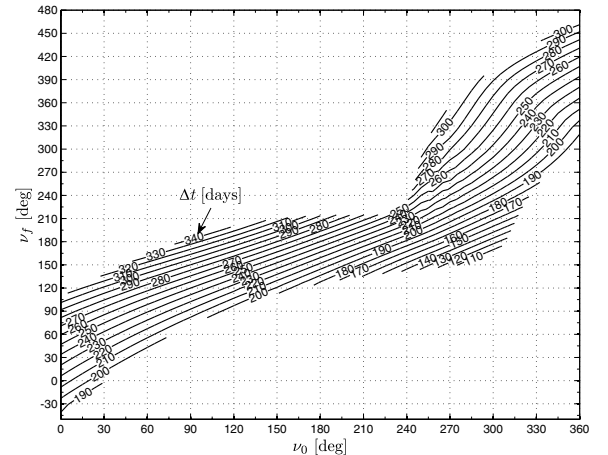
Figure 2b does not provide any information concerning the date corresponding to the optimal relative position between Earth and Apophis. Therefore, as a second step of our analysis, it is useful to investigate the sensitivity of the mission time with respect to the starting sailcraft position on Earth's orbit. This is possible by solving the constrained minimum time problem with $L(t_0)$ given, and $L(t_f)$ left free. The corresponding boundary conditions are those given in

**Fig. 1** Reference frames.

Eq. (29) except that pertaining $\lambda_L(t_0)$, which is now replaced by $L(t_0) = L_0$. Bearing in mind that the true longitude unambiguously characterizes the Earth's position along its orbit, L_0 defines the possible departure date.

The results are summarized in Fig. 3a for a number of values of the characteristic acceleration in the range $[0.5, 1.5] \text{ mm/s}^2$. As expected, the minimum mission times shown in Fig. 3a coincide with those of Fig. 2a in which $L(t_0)$ is unconstrained. For a given value of a_c , the mission times vary remarkably with the starting position on Earth's orbit. In particular, Fig. 3a shows that the differences between the maximum and minimum transfer times are always about 100 days for all of the values of characteristic acceleration.

For a given value of a_c , each function $\Delta t = f(v_0)$ has two minima: one (the global minimum) with a “steep slope” around it, the other (a local minimum) with “gentle” boundaries. For a given departure time t_0 (that is, for a given value of v_0), Fig. 3a provides a relationship between the characteristic acceleration and the corresponding minimum transfer time Δt . Clearly, a_c being fixed, the mission is feasible in the optimal time Δt , provided that Apophis's position (in terms of v_f) along its orbit at $t_f \triangleq t_0 + \Delta t$ coincides with that given in Fig. 3b. Otherwise, the transfer is still possible, but the mission would require a flight time greater than Δt . The information given in

**a) Flight times****b) Sailcraft initial and final positions****Fig. 2** Orbit-to-orbit transfer performance as a function of characteristic acceleration.**a) Flight times****b) Final spacecraft position on target orbit****Fig. 3** Mission performance as a function of starting position on Earth's orbit.

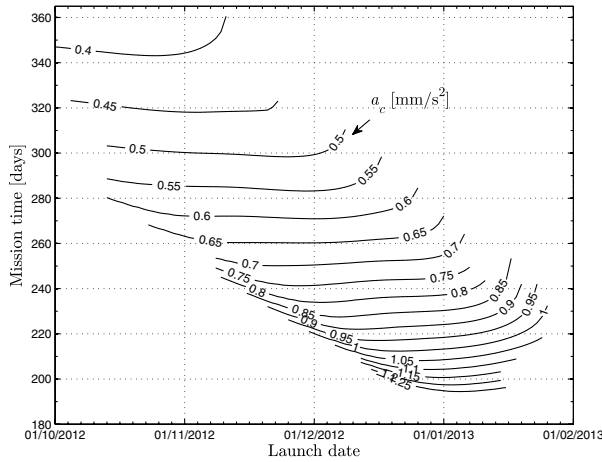


Fig. 4 Launch opportunities in 2012–2013 as a function of a_c .

Fig. 3 is useful for locating a possible launch window, that is, a triplet $(a_c, v_0, \Delta t)$ such that the value $v_o(t_f)$ coincides with v_f of Fig. 3b. This analysis falls within the third phase of our mission study.

Launch Windows

As stated previously, a realistic near-term mission option requires a solar sail with a characteristic acceleration on the order of 0.5 mm/s^2 . Assuming $a_c = 0.5 \text{ mm/s}^2$ as a reference value, we have investigated the most favorable launch windows before 2017 within one Earth–Apophis synodic period (about 7.769 years). A promising launch window is placed between the end of 2012 and the beginning of 2013. Within this time interval, the mission performance has been analyzed as a function of different values of a_c . The results are summarized in Fig. 4. The isocontour lines show a rather flat behavior, especially for characteristic accelerations in the range $a_c \in [0.4, 0.8] \text{ mm/s}^2$, thus implying the existence of wide launch opportunities having similar performance. Taking the minimum value of each isocontour line of Fig. 4 as a reference time for the corresponding mission opportunity, it is possible to calculate the differences in flight times with respect to the orbit-to-orbit optimal values of Fig. 2a. The results are summarized in Fig. 5, from which one sees that these differences vary between 50 and 85 days, with a percentage increase up to 75% (the latter situation corresponding to a characteristic acceleration $a_c = 1.25 \text{ mm/s}^2$).

Assuming $a_c = 0.5 \text{ mm/s}^2$, from Fig. 4, the optimal launch date is 27 November 2012 and the corresponding rendezvous time is 298.3 days. The whole mission is analyzed in Fig. 6, which summarizes the spacecraft trajectory, and in Fig. 7, which shows the clock and cone angle steering laws.

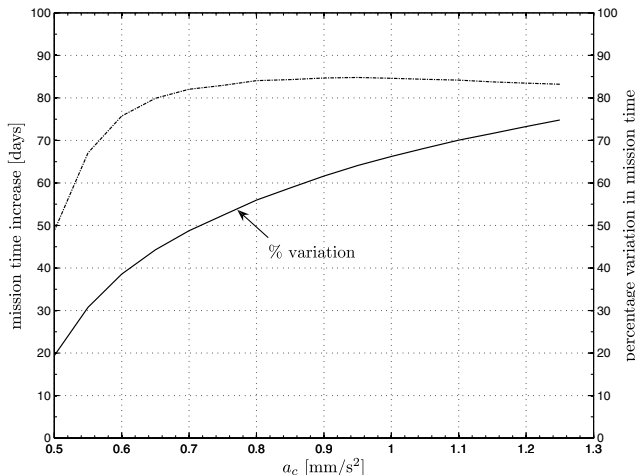


Fig. 5 Mission time increase with respect to the orbit-to-orbit optimal values.

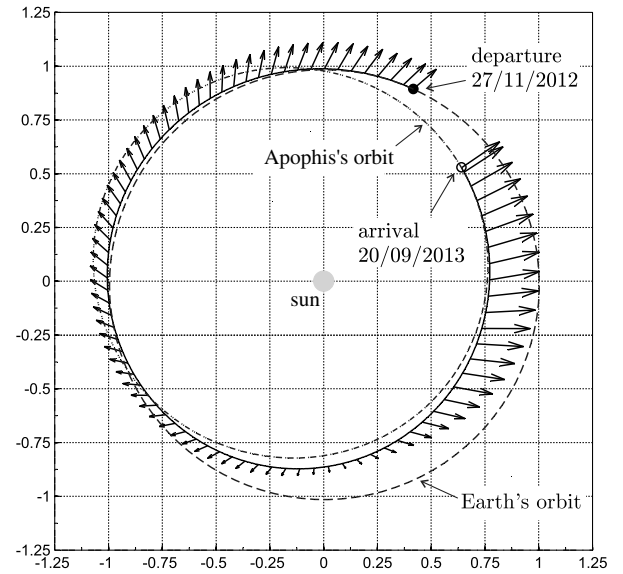
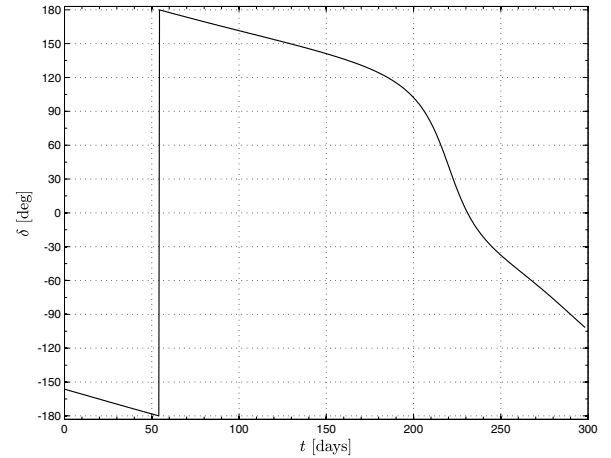
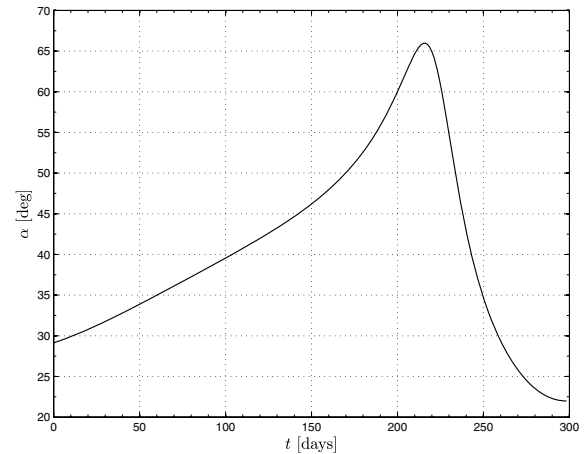


Fig. 6 Projection on the ecliptic plane of spacecraft trajectory and thrust profile for $a_c = 0.5 \text{ mm/s}^2$.



a) Sail clock angle δ



b) Sail cone angle α

Fig. 7 Time histories of sailcraft clock and cone angles for $a_c = 0.5 \text{ mm/s}^2$ (launch date 27 November 2012).

Comparison with Conventional Propulsion Systems

We are now interested in investigating the main performance differences that can be obtained when the Apophis's rendezvous is obtained using either a high-thrust or a solar electric propulsion

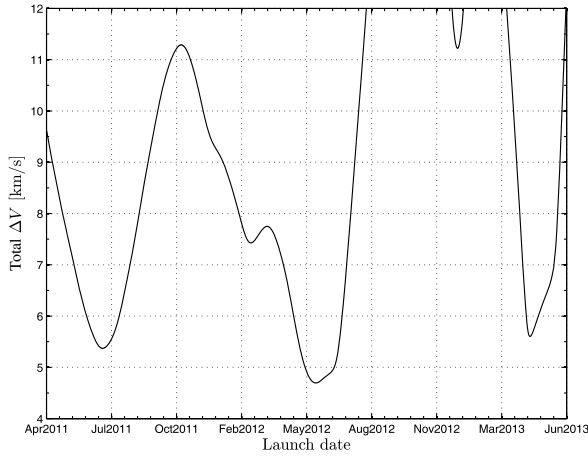


Fig. 8 Required ΔV as a function of launch date for two-impulse maneuver.

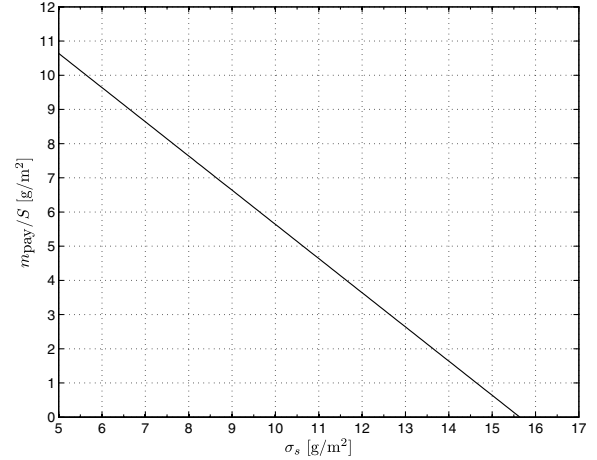


Fig. 10 Deliverable payload mass per unit area for $a_c = 0.5 \text{ mm/s}^2$.

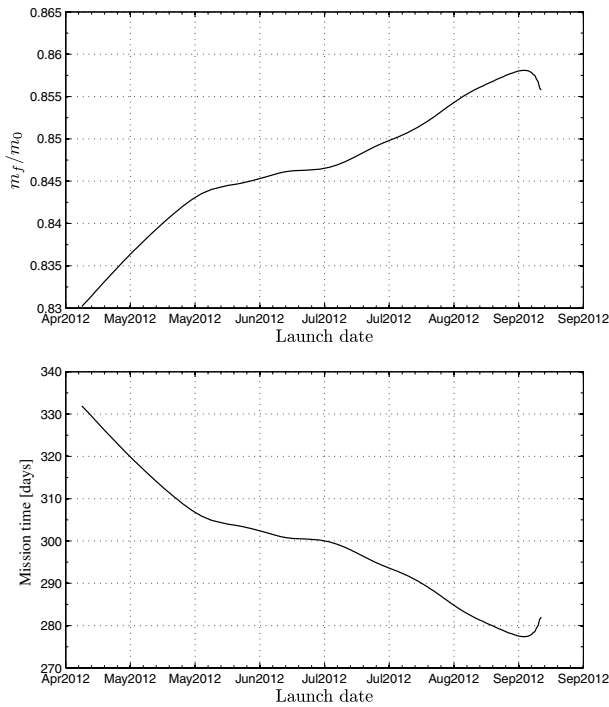


Fig. 9 Mission performance as a function of launch date for electric thruster option.

(SEP) system. For a reasonable comparison, we assume 1) that both solar sail and SEP system have the same payload mass, and 2) that the transfer times for both high-thrust and SEP systems are comparable to that found for the solar sail.

First, a targeting problem with a two-impulse maneuver is solved and the corresponding ΔV is found. Figure 8 shows the simulation results for the high-thrust propulsion system when a flight time of 300 days is considered. The optimal launch date is at the end of May 2012, with a $\Delta V = 4.70 \text{ km/s}$. Assuming a specific impulse $I_{sp} = 450 \text{ s}$, the rocket equation provides a mass fraction $m_f/m_0 = 0.3447$, corresponding to about 40% of that achievable with an electric propulsion system, as calculated in the succeeding Fig. 9.

The electric propulsion system needs a brief description regarding the main assumptions introduced in our simulations. The system has features comparable to that used in the Deep Space 1 mission, that is, a launch mass of 500 kg, $I_{sp} = 3100 \text{ s}$, and a maximum thrust level $T_{max} = 90 \text{ mN}$. The value of I_{sp} is constant during the whole mission: this amounts to neglecting any variation of available

thrust power with the sun distance. Also, the thrust is assumed to vary with continuity in the range $[0, T_{max}]$ and it may be freely oriented in the space. In this case, the control variables are the thrust level and its direction. Only missions with transfer times of about $\Delta t = 300$ days (comparable with that of solar sails) have been investigated. Because the time length is roughly given, the optimal SEP-based mission is obtained by looking for the minimum propellant consumption, that is, by maximizing the spacecraft final mass. Figure 9 shows the simulation results for the electric option in terms of mass ratio m_f/m_0 and flight time. The optimal launch window corresponds to the middle of September 2012, with a propellant consumption of 14.2% and a total flight time of 277 days. Note that the results of Fig. 9 can be combined by eliminating the launch time. It may be checked that one obtains a linear relationship between m_f/m_0 and the transfer time in the form

$$\frac{m_f}{m_0} = 1 - \frac{T_{max}}{g_0 I_{sp} m_0} \Delta t \quad (31)$$

Accordingly, the thruster is always on, and its level is maximum during the whole trajectory.

To estimate the deliverable payload mass and the characteristic dimension of a sailcraft, we use the simplified model of partitioning the total spacecraft mass into two components, the sail film and structure mass m_s and the payload mass m_{pay} , that is $m = m_s + m_{pay}$ [14]. Recall from Fig. 2a that the mission time is univocally established as a function of the sailcraft characteristic acceleration. For a given value of a_c , it may be shown [14] that the deliverable payload mass per unit area is a linear function of the sail assembly loading $\sigma_s \triangleq m_s/S$. Note that σ_s is a technological parameter and S is the sail total reflecting surface. Assuming $a_c = 0.5 \text{ mm/s}^2$, the payload mass can be estimated with the aid of Fig. 10. Consider, for example, three increasing payload mass cases corresponding to 50, 100, and 150 kg, respectively. Using a sail assembly loading $\sigma_s = 10 \text{ g/m}^2$, one obtains that the corresponding side lengths for a square sail are 87, 123, and 151 mm. A more accurate estimate (including the value of sail area, moments of inertia, and control system characteristics) can be obtained with the aid of the scalable sailcraft model developed by Murphy et al. [15]. It may be shown [16] that the main configuration parameters of a sailcraft with a characteristic acceleration $a_c = 0.53 \text{ mm/s}^2$ are a total mass of 300 kg, a square sail side length of 160 mm, and a payload mass of about 150 kg. A comparison with the previously analyzed SEP spacecraft configuration shows that a payload of 150 kg corresponds to a payload mass fraction of 30%. Of course, a smaller payload mass would reduce remarkably the side length of the solar sail, as previously noted.

In summary, for all of the three different propulsion systems considered in this analysis (solar sails, high-thrust, and electric propulsion) the optimal launch dates are in 2012. However, the solar sails seem to offer more flexible launch opportunities due to a

moderate sensitivity of mission time with respect to the optimal launch date.

Conclusions

Apophis has been used here as a practical example for investigating the potentialities of new mission concepts and as a starting point for a hypothetical space agency project aiming to tag an asteroid. In particular, the peculiarities offered by a solar-sail-based rapid mission toward Apophis have been investigated by analyzing the minimum time rendezvous missions as a function of the sail characteristic acceleration. A realistic near-term rapid mission option requires a solar sail with a characteristic acceleration not smaller than 0.4 mm/s^2 . An interesting launch opportunity aimed at reaching Apophis within 2017 is placed between the end of 2012 and the beginning of 2013. Assuming a solar sail with a characteristic acceleration of 0.53 mm/s^2 , the mission time is near 300 days, whereas the sailcraft requires a total mass of about 300 kg, a square sail side length of 160 mm, and a payload mass of 150 kg. Smaller sail dimensions (that is, a side length of 90 m) can be obtained using a reduced payload mass of about 50 kg. The latter value is consistent with the payload mass of NASA's Dawn spacecraft.

Values of sail dimensions of about 100 mm or more are certainly remarkable, and are not currently available. Also, the deployment and control of such a large solar sail in space will not be a simple task. However, different near-term solar sailing missions requiring large solar sail side lengths and the associated solar sail technologies are being developed. In particular, a 160-m solar sail will be required for the Solar Polar Imager mission, which is currently envisaged by NASA.

Launch windows for spacecraft powered by either electric or high-thrust systems have been also investigated. Optimal launch opportunities in terms of propellant consumption have been found. For all of the three different propulsion systems, the optimal launch dates are located in 2012. An interesting feature of solar sails is their capability of offering wide launch opportunities when compared to more conventional propulsion systems. This makes a solar sail an attractive option for future missions toward small celestial bodies.

Appendix

The transformations from modified equinoctial elements \mathbf{x} [see Eq. (5)] to spacecraft position and velocity (with respect to the heliocentric-ecliptic inertial frame \mathcal{T}_\odot), are

$$[\mathbf{r}]_{\mathcal{T}_\odot} = \frac{r}{(1+h^2+k^2)} \begin{bmatrix} (1+h^2-k^2)\cos L + 2hk\sin L \\ (1-h^2+k^2)\sin L + 2hk\cos L \\ 2h\sin L - 2k\cos L \end{bmatrix} \quad (\text{A1})$$

$$[\mathbf{v}]_{\mathcal{T}_\odot} = -\frac{\sqrt{\mu_\odot/p}}{1+h^2+k^2} \begin{bmatrix} (\sin L + g)(h^2 - k^2 + 1) - 2hk(\cos L + f) \\ (\cos L + f)(h^2 - k^2 - 1) + 2hk(\sin L + g) \\ -2h(\cos L + f) - 2k(\sin L + g) \end{bmatrix} \quad (\text{A2})$$

where $r = p/(1+f\cos L + g\sin L)$.

The transformations from modified equinoctial elements to classical orbital elements are obtained from the following relationships:

$$a = \frac{p}{1-f^2-g^2} \quad (\text{A3})$$

$$e = \sqrt{f^2 + g^2} \quad (\text{A4})$$

$$i = 2 \arctan \sqrt{h^2 + k^2} \quad (\text{A5})$$

$$\sin \omega = gh - fk, \quad \cos \omega = fh + gk \quad (\text{A6})$$

$$\sin \Omega = k, \quad \cos \Omega = h \quad (\text{A7})$$

$$v = L - \Omega - \omega \quad (\text{A8})$$

References

- [1] Morrison, D., Harris, A. W., Sommer, G., Chapman, C. R., and Carusi, A., "Dealing with the Impact Hazard," *Asteroids III*, edited by W. Bottke, A. Cellino, P. Paolicchi, and R. P. Binzel, Univ. of Arizona Press, Tucson, AZ, 2002, pp. 739–754.
- [2] Farinella, P., Foschini, L., Froeschlé, C., Gonczi, R., Jopek, T. J., Longo, G., and Michel, P., "Probable Asteroidal Origin of the Tunguska Cosmic Body," *Astronomy and Astrophysics*, Vol. 377, Oct. 2001, pp. 1081–1097.
doi:10.1051/0004-6361:20011054
- [3] Mengali, G., and Quarta, A. A., "Optimal Three-Dimensional Interplanetary Rendezvous Using Nonideal Solar Sail," *Journal of Guidance, Control, and Dynamics*, Vol. 28, No. 1, Jan.–Feb. 2005, pp. 173–177.
doi:10.2514/1.8325
- [4] Dachwald, B., Mengali, G., Quarta, A. A., and Macdonald, M., "Parametric Model and Optimal Control of Solar Sails with Optical Degradation," *Journal of Guidance, Control, and Dynamics*, Vol. 29, No. 5, Sept.–Oct. 2006, pp. 1170–1178.
doi:10.2514/1.20313
- [5] Walker, M. J. H., Owens, J., and Ireland, B., "A Set of Modified Equinoctial Orbit Elements," *Celestial Mechanics*, Vol. 36, Aug. 1985, pp. 409–419.
doi:10.1007/BF01227493
- [6] Walker, M. J., "Erratum: A Set of Modified Equinoctial Orbit Elements," *Celestial Mechanics*, Vol. 38, April 1986, pp. 391–392.
doi:10.1007/BF01238929
- [7] Betts, J. T., "Very Low-Thrust Trajectory Optimization Using a Direct SQP Method," *Journal of Computational and Applied Mathematics*, Vol. 120, No. 1, Aug. 2000, pp. 27–40.
doi:10.1016/S0377-0427(00)00301-0
- [8] Wie, B., "Thrust Vector Control of Solar Sail Spacecraft," *AIAA Guidance, Navigation, and Control Conference and Exhibit*, AIAA Paper 2005-6086, Aug. 2005.
- [9] Patel, P., Scheeres, D., and Gallimore, A., "Maximizing Payload Mass Fractions of Spacecraft for Interplanetary Electric Propulsion Missions," *Journal of Spacecraft and Rockets*, Vol. 43, No. 4, July–Aug. 2006, pp. 822–827.
doi:10.2514/1.17433
- [10] Bryson, A. E., and Ho, Y. C., *Applied Optimal Control*, Hemisphere, New York, 1975, Chap. 2, pp. 71–89.
- [11] Forsythe, G. E., Michael, A. M., and Moler, C. B., *Computer Methods for Mathematical Computations*, Prentice-Hall, Englewood Cliffs, NJ, 1977, pp. 192–235.
- [12] Standish, E. M., "JPL Planetary and Lunar Ephemerides, DE405/LE405," Interoffice Memo IOM312.F-98-048, Jet Propulsion Lab., 26 Aug. 1998, <http://iau-comm4.jpl.nasa.gov/de405iom/de405iom.pdf> [cited 28 Aug. 2008].
- [13] Standish, E. M., and Fienga, A., "Accuracy Limit of Modern Ephemerides Imposed by the Uncertainties in Asteroid Masses," *Astronomy and Astrophysics*, Vol. 384, Feb. 2002, pp. 322–328.
doi:10.1051/0004-6361:20011821
- [14] Mengali, G., and Quarta, A. A., "Solar-Sail-Based Stopover Cyclers for Cargo Transportation Missions," *Journal of Spacecraft and Rockets*, Vol. 44, No. 4, July–Aug. 2007, pp. 822–830.
doi:10.2514/1.24423
- [15] Murphy, D. M., Murphey, T. W., and Gierow, P. A., "Scalable Solar-Sail Subsystem Design Concept," *Journal of Spacecraft and Rockets*, Vol. 40, No. 4, July–Aug. 2003, pp. 539–547.
doi:10.2514/2.3975
- [16] Wie, B., "Solar Sailing Kinetic Energy Interceptor (KEI) Mission for Impacting and Deflecting Near-Earth Asteroids," *AIAA Guidance, Navigation, and Control Conference and Exhibit*, AIAA Paper 2005-6175, Aug. 2005.